

# Complementary optical and nuclear imaging of caspase-3 activity using combined activatable and radio-labeled multimodality molecular probe

Hyeran Lee,<sup>a</sup> Walter J. Akers,<sup>a</sup> Philip P. Cheney,<sup>a</sup> W. Barry Edwards,<sup>a</sup> Kexian Liang,<sup>a</sup> Joseph P. Culver,<sup>a</sup> and Samuel Achilefu<sup>a,b,\*</sup>

<sup>a</sup>Washington University, School of Medicine, Department of Radiology, St. Louis, Missouri 63110

<sup>b</sup>Washington University, Department of Biochemistry and Molecular Biophysics, St. Louis, Missouri 63110

**Abstract.** Based on the capability of modulating fluorescence intensity by specific molecular events, we report a new multimodal optical-nuclear molecular probe with complementary reporting strategies. The molecular probe (LS498) consists of tetraazacyclododecanetetraacetic acid (DOTA) for chelating a radionuclide, a near-infrared fluorescent dye, and an efficient quencher dye. The two dyes are separated by a cleavable peptide substrate for caspase-3, a diagnostic enzyme that is upregulated in dying cells. LS498 is radiolabeled with <sup>64</sup>Cu, a radionuclide used in positron emission tomography. In the native form, LS498 fluorescence is quenched until caspase-3 cleavage of the peptide substrate. Enzyme kinetics assay shows that LS498 is readily cleaved by caspase-3, with excellent enzyme kinetic parameters  $k_{\text{cat}}$  and  $K_M$  of  $0.55 \pm 0.01 \text{ s}^{-1}$  and  $1.12 \pm 0.06 \mu\text{M}$ , respectively. In mice, the initial fluorescence of LS498 is ten-fold less than control. Using radiolabeled <sup>64</sup>Cu-LS498 in a controlled and localized *in vivo* model of caspase-3 activation, a time-dependent five-fold NIR fluorescence enhancement is observed, but radioactivity remains identical in caspase-3 positive and negative controls. These results demonstrate the feasibility of using radionuclide imaging for localizing and quantifying the distribution of molecular probes and optical imaging for reporting the functional status of diagnostic enzymes. © 2009 Society of Photo-Optical Instrumentation Engineers. [DOI: 10.1117/1.3207156]

Keywords: optical imaging; nuclear imaging; scintigraphy; caspase-3; near-infrared fluorescence resonance energy transfer.

Paper 09206LR received May 22, 2009; revised manuscript received Jun. 26, 2009; accepted for publication Jun. 30, 2009; published online Aug. 25, 2009.

## 1 Introduction

Multimodal imaging has been driven by the realization that no single imaging method has a complete solution to the multi-

faceted challenges of disease diagnosis and prognosis. For example, the addition of molecular imaging to the current functional and structural imaging methods requires procedures that report molecular events without loss of anatomical information. A common practice today is to combine methods with high spatial resolution such as magnetic resonance imaging (MRI), x-ray computed tomography (CT), and ultrasound with those with high detection sensitivity such as positron emission tomography (PET) and diffuse optical tomography (DOT).

A less utilized multimodal strategy is the combination of two functional or molecular imaging methods, such as optical-nuclear multimodal imaging. As summarized in a recent report, there are many reasons to utilize this hybrid of two modalities with similarly high detection sensitivity.<sup>1</sup> For example, although combining molecular optical contrasts with MRI or CT provides coregistered reference anatomy, the disparate contrast mechanisms present a barrier to integrating the imaging data. Because of the high sensitivity of both PET and optical methods and the compatibility of their imaging agents, we and others have reported the use of monomolecular multimodality imaging agents (MOMIAs) for combined nuclear-optical imaging studies.<sup>2,3</sup> These studies have established the equivalence or identical origin of signals from both contrast sources through image coregistration. The dual optical-nuclear imaging approach has been extended to nanomaterials, where PET and optical imaging have been combined to improve quantitative accuracy.<sup>4,5</sup>

In this study, we sought to develop a complementary imaging strategy that would harness the strengths of NIR fluorescence and nuclear imaging methods. To achieve this goal, we hypothesized that incorporating an activatable fluorescent molecular system into a radio-labeled cleavable peptide would provide a unique opportunity to fuse imaging data with identical pharmacokinetics but different reporting strategies. Accordingly, we prepared a multifunctional molecular probe (LS498) with persistent radionuclide signal and activatable fluorescence in response to a specific molecular process.

## 2 Methods

The peptide backbone, metal chelating group DOTA, and NIR fluorescent dye<sup>6</sup> used in LS498 (Fig. 1), were assembled as described previously.<sup>2</sup> The NIR fluorescent quencher, IR dye QC-1 (Licor, Lincoln, Nebraska), was incorporated into the multifunctional peptide at room temperature in phosphate buffered saline (PBS) for 24 h. The purified LS498 (5  $\mu\text{g}$ , 1.3 nmol) was radio-labeled by heating (60 °C, 0.5 h) with <sup>64</sup>Cu (470  $\mu\text{Ci}$ ) in aqueous buffer (100-mM NH<sub>4</sub>OAc, pH 5.5). The caspase-3 enzyme kinetic parameters were determined as previously described.<sup>7,8</sup>

As a model of tumor-related caspase activity, plastic tubes containing <sup>64</sup>Cu-LS498 (50  $\mu\text{L}$ , 1  $\mu\text{M}$ ) and either 260-pM caspase-3 or 5- $\mu\text{M}$  bovine serum albumin (BSA) in assay buffer were implanted subcutaneously in opposite flanks of the mouse. Multimodal imaging and region of interest (ROI) analysis of fluorescence (755-nm excitation, 830-nm emission), x-ray, and scintigraphy were performed with the IS4000MM (Carestream Health, New Haven, Connecticut) as previously described.<sup>2</sup>

\*Address all correspondence to: Samuel Achilefu, E-mail: achilefu@mir.wustl.edu

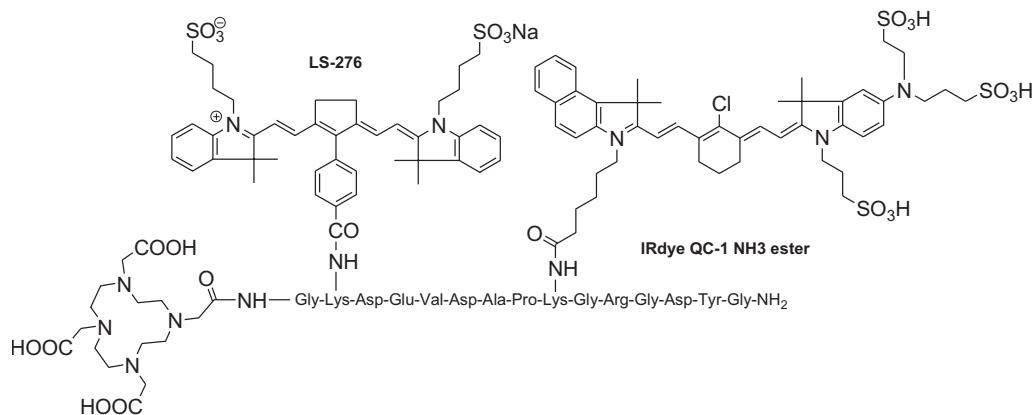


Fig. 1 Structure of caspase-3 activatable optical-nuclear molecular probe (LS498).

### 3 Results and Discussion

#### 3.1 Development of Caspase-3 Activatable Probe for Dual Optical-Nuclear Imaging

A multifunctional peptide-based molecular probe LS498 (Fig. 1) was designed and prepared for use in this study. Because of the need to monitor the response of diseased tissue to treatment and the implication of caspase-3 in early cell death,<sup>7</sup> LS498 was specifically developed to report the activity of this diagnostic enzyme. To accomplish this goal, we used a fluorescence resonance energy transfer (FRET) system, where the fluorescence of a NIR dye was efficiently quenched with wide-spectrum quencher dye. Since the tetrapeptide sequence, aspartic acid-glutamic-acid-valine-aspartic acid (DEVD), is an established substrate for caspases-3,<sup>7</sup> we incorporated this peptide sequence between the two dyes. Cleavage of the DEVD peptide results in fluorescence enhancement that can be used to monitor enzyme activity.<sup>7,8</sup> In the quenched state, it is not feasible to image the distribution of the molecular probe in tissue prior to enzyme cleavage. Moreover, lack of fluorescence enhancement may be due to inadequate delivery of the molecular probe to the target tissue, a situation that could result in false-negative outcomes. To address this issue, LS498 was labeled with <sup>64</sup>Cu, a positron emitter with half-life of 12.8 h. This radionuclide is widely used in PET imaging of molecular processes in small animals and humans.<sup>9</sup> After HPLC purification, LS498 was labeled with <sup>64</sup>Cu at high specific activity (360 Ci/mmol) and purity (>99%). In previous work with <sup>64</sup>Cu-DOTA-c(RGDyK), specific activities ranged from 200 to 500 Ci/mmol and receptor-specific tumor accumulation allowed for α<sub>v</sub>β<sub>3</sub>-positive tumor visualization by small animal PET.<sup>10</sup> Therefore, the observed specific activity in LS498 is adequate for receptor targeted tumor imaging *in vivo*.

#### 3.2 Caspase-3 Enzyme Kinetics

The feasibility of applying a reporter of proteolytic activity to *in-vivo* imaging depends on how fast the substrate is processed by the enzyme before being washed away from the target site. The kinetic parameters,  $k_{cat}$  and  $K_M$ , are measurable indicators of how well a substrate is processed by an enzyme. Our study shows that LS498 was readily cleaved by caspase-3 and displayed classic Michaelis-Menten kinetics (Fig. 2) with enzyme kinetic parameters  $k_{cat}$  and  $K_M$  of

$0.55 \pm 0.01 \text{ s}^{-1}$  and  $1.12 \pm 0.06 \mu\text{M}$ , respectively. The observed  $k_{cat}$  and  $K_M$  compares favorably with standard substrates Ac-DEVD-AMC ( $k_{cat}=0.75 \text{ s}^{-1}$ ,  $K_M=9.7 \mu\text{M}$ ) and Ac-DEVD-pNA ( $k_{cat}=0.55 \pm 0.01 \text{ s}^{-1}$ ,  $K_M=11 \mu\text{M}$ ). The  $k_{cat}/K_M$  ratio, which measures the performance constant of an enzyme for a substrate, was found to be  $4.91 \times 10^5 \text{ s}^{-1}\text{M}^{-1}$ .

#### 3.3 In-Vivo Imaging of LS-498 Distribution and Model of Caspase-3 Activation

LS498 was designed to prevent fluorescence emission prior to activation by caspase-3. To assess if this goal was met, we compared the fluorescence emission of LS498 to a control analog. The control peptide lacks a quencher dye, thereby reporting the maximum fluorescence intensity of a completely cleaved LS498. Intravenous injection of the two molecular probes in healthy mice showed that fluorescence was hardly detectable in the mouse injected with LS498 and remained lower than that of the control probe up to 24-h postinjection. Immediately after injection (30 min), the fluorescence intensity was at least ten-fold less for LS498 relative to control [Fig. 3(a)]. After 24 h, both molecular probes had similar low fluorescence intensity (data not shown), approaching the detection limit of our imaging system. Interestingly, the kidneys were visible at 24 h in both mice, suggesting a possible degradation of LS498 after prolonged retention in this organ. Al-

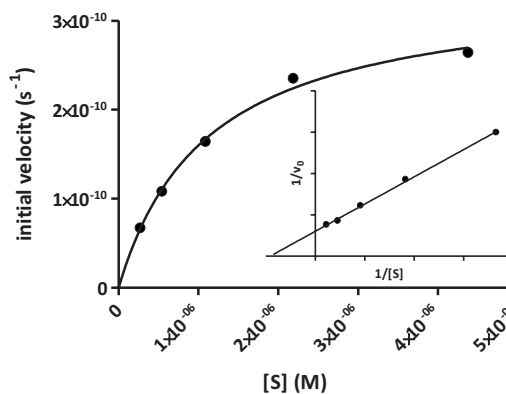
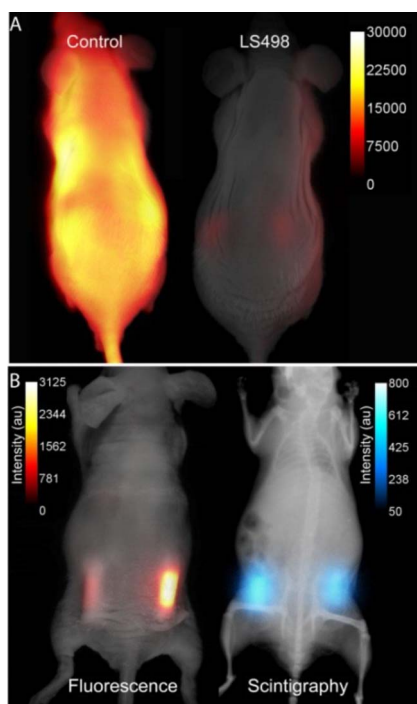


Fig. 2 Nonlinear fit of initial velocity with respect to substrate concentration and the corresponding Lineweaver-Burk plot (insert). Substrate concentrations varied from 270 nM to 35 μM.



**Fig. 3** Imaging of multifunctional molecular probe in mice. (a) *In-vivo* distribution of LS498 (right) and nonquenched control analog (left) in mice at 30 min after intravenous injection of the imaging agents. Fluorescence of the activatable probe was efficiently quenched by greater than 10-fold relative to the nonquenched control. (b) Multimodal fluorescence (left) and scintigraphic (right) imaging of a mouse with subcutaneously implanted tubes containing  $^{64}\text{Cu}$ -LS498 with BSA (left side) or caspase-3 (right side) 2 h after implantation. Tubes were implanted subcutaneously (about 1 mm) below the surface of the skin. Radioactivity is always “on” but fluorescence enhancement depends on the presence of caspase-3. The ratio of fluorescence intensity for the caspase-3 sample was 4.2 times greater than the control sample, and this ratio increased to 5.6-fold after normalizing to radioactivity.

ternatively, it is also possible that the kidneys express residual levels of caspase-3 that were responsible for the observed fluorescence enhancement.

To evaluate the feasibility of imaging caspase-3 activity in small animals, we developed an artificial model of subcutaneous tumor in mice. Two tubes containing radiolabeled  $^{64}\text{Cu}$ -LS498 were each mixed with either caspase-3 or bovine serum albumin (BSA) to mimic tissues expressing caspase-3 versus control, respectively. Expectedly, the fluorescence of caspase-3 containing tube increased with time, reaching a plateau after 4 h. In contrast, the BSA control tube did not show any fluorescence enhancement up to 24 h [Fig. 3(b)]. In contrast to the scintigraphy image where both tubes had similar radioactivity, the optical imaging clearly distinguished caspase-3 positive from the negative tube based on differences in their fluorescence intensity. These findings demonstrate the feasibility of using LS498 to report concentration through nuclear contrast and enzyme activity through optical contrast in a controlled *in-vivo* context. To be effective in a tumor model, LS498 has to be internalized in cells where the cytosolic caspase-3 resides. Cytosolic delivery could be

achieved by incorporating cell-permeating peptides to LS498 or via a receptor-mediated endocytosis mechanism that is coupled with endosomal disrupting peptides.

In conclusion, this work summarizes our ongoing efforts toward the development of multimodality imaging agents for combined optical and nuclear molecular imaging of diseased tissues. In this study, the always “on” nuclear signal is useful for quantifying and localizing the distribution of the probe, while the optical imaging reports the functional status of a target molecular event. Both *in-vitro* and *in-vivo* results demonstrate the feasibility of using this approach to image molecular processes. Although we used caspase-3 as a model for this study, the complementary contrast strategy is applicable to imaging the functional status of most enzymes. Studies are in progress to demonstrate the utility of this new imaging strategy in animal disease models.

#### Acknowledgments

We thank Licor for the generous gift of the quencher dye used in this study. This study was funded in part by the National Institutes of Health (R01 CA109754 and R01EB008458).

#### References

1. J. Culver, W. Akers, and S. Achilefu, “Multimodality molecular imaging with combined optical and SPECT/PET modalities,” *J. Nucl. Med.* **49**, 169–172 (2008).
2. W. B. Edwards, W. J. Akers, Y. Ye, P. P. Cheney, S. Bloch, B. Xu, R. Laforest, and S. Achilefu, “Multimodal imaging of integrin receptor-positive tumors by bioluminescence, fluorescence, gamma scintigraphy, and single-photon emission computed tomography using a cyclic RGD peptide labeled with a near-infrared fluorescent dye and a radionuclide,” *Mol. Imaging* **8**, 101–110 (2009).
3. C. Li, W. Wang, Q. Wu, S. Ke, J. Houston, E. Sevick-Muraca, L. Dong, D. Chow, C. Charnsangavej, and J. G. Gelovani, “Dual optical and nuclear imaging in human melanoma xenografts using a single targeted imaging probe,” *Nucl. Med. Biol.* **33**, 349–358 (2006).
4. W. Cai, K. Chen, Z. B. Li, S. S. Gambhir, and X. Chen, “Dual-function probe for PET and near-infrared fluorescence imaging of tumor vasculature,” *J. Nucl. Med.* **48**, 1862–1870 (2007).
5. F. Duconge, T. Pons, C. Pestourie, L. Herin, B. Theze, K. Gombert, B. Mahler, F. Hinnen, B. Kuhnast, F. Dolle, B. Dubertret, and B. Tavittian, “Fluorine-18-labeled phospholipid quantum dot micelles for *in vivo* multimodal imaging from whole body to cellular scales,” *Bioconjugate Chem.* **19**, 1921–1926 (2008).
6. H. Lee, M. Y. Berezin, M. Henary, L. Streckowski, and S. Achilefu, “Fluorescence lifetime properties of near-infrared cyanine dyes in relation to their structures,” *J. Photochem. Photobiol., A* **200**, 438–444 (2008).
7. K. E. Bullock, D. Maxwell, A. H. Kesarwala, S. Gammon, J. L. Prior, M. Snow, S. Stanley, and D. Piwnica-Worms, “Biochemical and *in vivo* characterization of a small, membrane-permeant, caspase-activatable far-red fluorescent peptide for imaging apoptosis,” *Biochem. J.* **46**, 4055–4065 (2007).
8. Z. Zhang, J. Fan, P. P. Cheney, M. Y. Berezin, W. B. Edwards, W. J. Akers, D. Shen, K. Liang, J. P. Culver, and S. Achilefu, “Activatable molecular systems using homologous near-infrared fluorescent probes for monitoring enzyme activities *in vitro*, *in cellulo*, and *in vivo*,” *Mol. Pharmaceutics* **6**, 416–427 (2009).
9. M. R. Lewis, M. Wang, D. B. Axworthy, L. J. Theodore, R. W. Mallet, A. R. Fritzberg, M. J. Welch, and C. J. Anderson, “*In vivo* evaluation of pretargeted  $^{64}\text{Cu}$  for tumor imaging and therapy,” *J. Nucl. Med.* **44**, 1284–1292 (2003).
10. X. Chen, R. Park, M. Tohme, A. H. Shahinian, J. R. Bading, and P. S. Conti, “MicroPET and autoradiographic imaging of breast cancer alpha v-integrin expression using  $^{18}\text{F}$ - and  $^{64}\text{Cu}$ -labeled RGD peptide,” *Bioconjugate Chem.* **15**, 41–49 (2004).